In Vitro Metabolism of a Model Cyclopropylamine to Reactive Intermediate: Insights into Trovafloxacin-Induced Hepatotoxicity

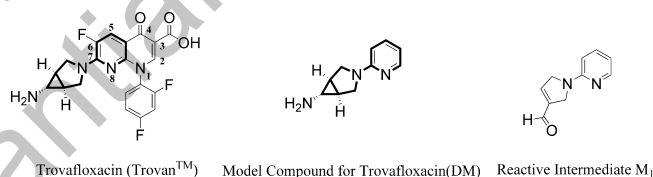Qin Sun, Ran Zhu, Frank W. Foss, Jr.,[†] and Timothy L. Macdonald*

Department of Chemistry, University of Virginia, Charlottesville, Virginia 22901

Trovafloxacin (Trovan) is a fluoroquinolone antibiotic drug with a long half-life and broad-spectrum activity. Since its entry into the market in 1998, trovafloxacin has been associated with numerous cases of hepatotoxicity, which has limited its clinical usefulness. Trovafloxacin possesses two substructural elements that have the potential to generate reactive intermediates: a cyclopropylamine moiety and a difluoroanilino system. The results presented here describe the in vitro metabolic activation of a synthetic drug model (DM) of trovafloxacin that contains the cyclopropylamine moiety. Cyclopropylamine can be oxidized to reactive ring-opened products—a carbon-centered radical and a subsequently oxidized α,β-unsaturated aldehyde. Experiments with monoamine oxygenases, horseradish peroxidase, flavin monooxygenase 3, and cDNA-expressed P450 isoenzymes revealed that P450 1A2 oxidizes DM to a reactive α,β-unsaturated aldehyde, M_1. Furthermore, myeloperoxidase (MPO) was also demonstrated to oxidize DM in the presence of chloride ion to produce M_1. DM proved to be a suicide inhibitor of MPO while showing no inhibition of P450 1A2. The structure of the reactive metabolite was confirmed by LC-MS/MS analysis by comparison with a synthetic standard. M_1 was further shown to react with glutathione and the related thiol nucleophile, 4-bromobenzyl mercaptan, suggesting the potential of this intermediate to react with protein nucleophiles. In summary, these data provide evidence that trovafloxacin-induced hepatotoxicity may be mediated through the oxidation of the cyclopropylamine substructure to reactive intermediates that may form covalent adducts to hepatic proteins, resulting in damage to liver tissue.

Introduction

Trovafloxacin, (1α,5α,6α)-7-(6-amino-3-azabicyclo[3.1.0]hex-3-yl)-1-(2,4-difluorophenyl)-6-(fluoro-1,4-dihydro-4-oxo-1,8-naphthyridine-3-carboxylic acid) (TVX) (Figure 1), is a novel fourth-generation fluoroquinolone with enhanced in vitro activity against Gram-positive and Gram-negative organisms, atypical pathogens, and anaerobes (*1–3*). Its pharmacokinetic profile enables once-daily (oral or intravenous) dosing for all indications (*4*). Before its approval in 1997, clinical trials in 7000 patients found no cases of hepatic failure or death associated with the use of TVX. Since its approval for marketing in 1998, 150 cases (occurring in 0.006% of patients) of clinically symptomatic liver toxicity have been reported, including at least 14 cases of acute liver failure. Four patients required liver transplants, and an additional five died of liver-related illness (*5*). These rare but severe liver injuries led to the withdrawal of TVX (Trovan) from the market in some countries and a black-box warning with intensive monitoring requirements in the United States (*6*). Clinical reports characterized the hepatotoxicity of TVX as an idiosyncratic drug reaction (IDR)[1] since it was unpredictable and possibly immunoallergic (*7*).

* To whom correspondence should be addressed. Tel: 434-924-7718. Fax: 434-982-2302. E-mail: tlm@virginia.edu.

† Current address: Department of Chemistry, Columbia University, New York, New York 10027.

[1] Abbreviations: *C*-HAT, carbon−hydrogen atom transfer; DM, the cyclopropyl amine-containing drug model of trovafloxacin; FMO3, flavin monooxygenase 3; GSH, reduced glutathione; HLMs, human liver microsomes; HRP, horseradish peroxidase; IDR, idiosyncratic drug reaction; LPS, lipopolysaccharide; M_1, the α,β-unsaturated aldehyde metabolite of the drug model system; MAO-A/B, monoamine oxygenase-A/B; MPO, myeloperoxidase; *N*-HAT, nitrogen−hydrogen atom transfer; SET, single electron transfer; TVX, trovafloxacin.

Figure 1. Chemical structure of TVX, DM, and M_1. The bold lines highlight the similarities between TVX and DM.

Structurally, TVX contains a cyclopropylamine moiety at the *C*-7 position of the fluoroquinolone scaffold. Cyclopropylamines have been widely applied as mechanistic probes of cytochrome P450s and other oxidative enzymes during the past three decades. P450 enzymes prefer second and tertiary cyclopropylamines as substrates (*8–11*). Most primary cyclopropylamines studied are oxidized by monoamine oxygenases (MAO-A/B) (*12–15*). These enzymes are therefore possible candidates for generating reactive metabolites that may contribute to the IDR of TVX. Another enzyme that is often investigated in mechanistic studies of drug bioactivation is horseradish peroxidase (HRP), which has been shown to oxidize amines through a single electron transfer (SET) mechanism. Although HRP is generally restricted to the oxidation of aromatic amines instead of aliphatic amines due to the relatively low redox potential of its activated state, *trans*-2-phenylcyclopropylamine has been reported to be a substrate and suicide inhibitor of HRP (*16*). In addition, the nonliver enzyme—myeloperoxidase (MPO)—also deserves investigation, since neutrophils, which release MPO when activated, have been associated with the IDR of TVX in animal models (*17*).

Cyclopropylamine-containing substrates have been widely utilized in mechanistic studies of oxidative enzymes, since the observation that cyclopropylbenzylamine and its methyl ana-

Scheme 1. Proposed SET Mechanism for P450-Mediated Oxidation of TVX to Reactive Carbon-Centered Radical or to α,β-Unsaturated Aldehyde
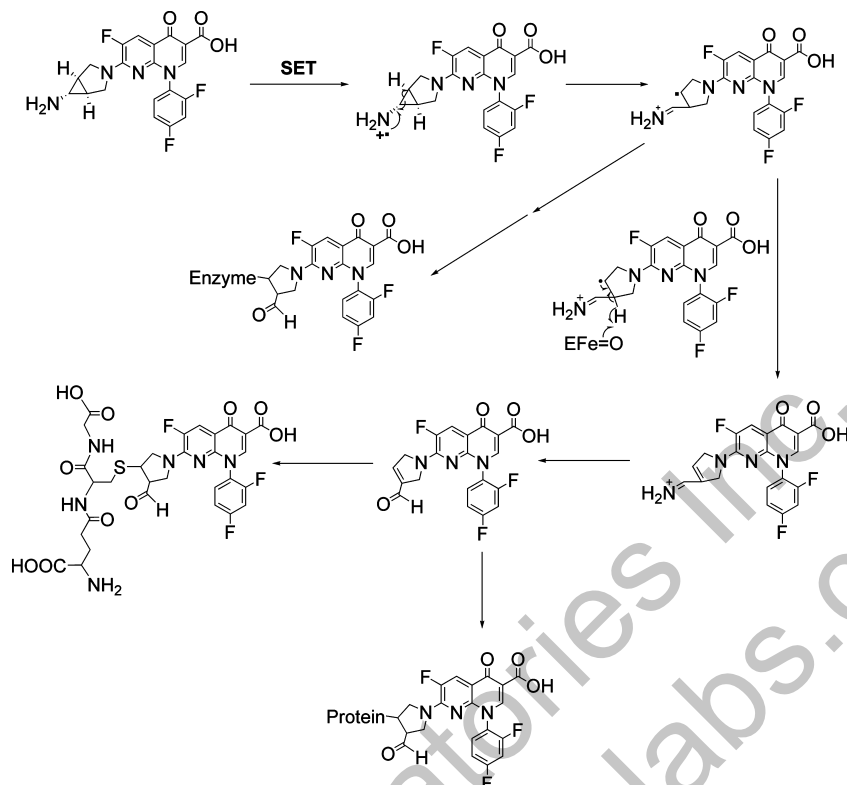
logue (1-methylcyclopropyl) benzylamine are equally efficient in suicide inhibition of P450 enzymes (*8*). According to the SET mechanism proposed to rationalize this observation, the cyclopropylamine structure is oxidized by P450 enzymes to produce a nitrogen radical cation, followed by rapid ring opening to form a highly reactive carbon-centered radical. This radical species could react with another radical source present at the catalytic site of the enzyme. Alternatively, the carbon-centered radical can be subsequently oxidized to the corresponding α,β-unsaturated iminium ion, which can be hydrolyzed to an α,β-unsaturated aldehyde. The metabolic study of cyclopropylamines implicates a rational mechanism of toxicity for TVX (Scheme 1). The cyclopropylamine moiety of TVX can be oxidized to reactive carbon-centered radical or an α,β-unsaturated aldehyde. Conjugation of either metabolite with reduced glutathione (GSH) or essential liver proteins could lead to the hepatoxicity of TVX.

Although the SET mechanism is prevailing for explanation of oxidation of cyclopropylamines by P450 enzymes as compared with the traditional *C*-HAT mechanism, neither mechanism explains all of the observations from the oxidation of cyclopropylamines. On the basis of the fact that *N*-benzyl-*N*-cyclopropyl-*N*-methylamine was found not to inactivate P450 and not to give rise to 3-hydroxypropionaldehyde as a metabolite without first undergoing oxidative *N*-demethylation, Hanzlik et al. proposed a *N*-HAT mechanism for the P450 oxidation of cyclopropylamines (*11*). The mechanism involves hydrogen abstraction at the N−H bond. This yields a neutral aminyl radical that could undergo rapid ring opening, leading to either enzyme inactivation or α,β-unsaturated aldehyde formation. This mechanism is illustrated in Scheme 2 for the drug model (DM).
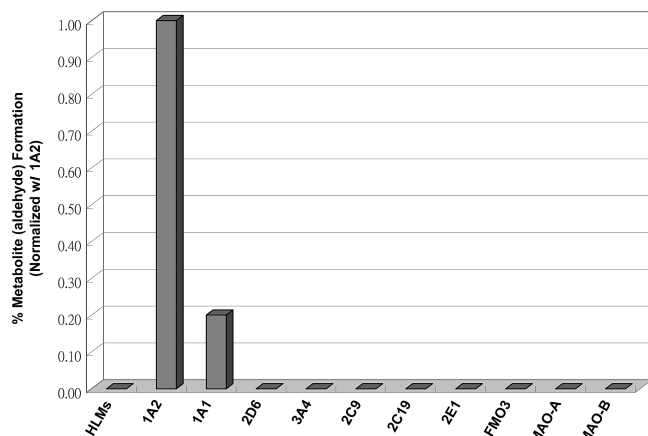
Cyclopropylamine is the most suspected substructure responsible for the hepatotoxicity of TVX. Although the difluoroanilino functional group has been suggested to be the responsible position (*18*), experimental evidence does not exist. To exclude interferences from other possible oxidizable positions, especially the difluoroanilino moiety, we have utilized a cyclopropylamine-containing model compound, the DM, to exclusively probe the potential of the cyclopropylamine substructure to contribute to the hepatotoxicity of TVX (Figure 1). Thus, the objectives of this study are (i) the detection and structural characterization of novel reactive intermediate(s) resulting from in vitro enzyme metabolism of a TVX model that contains its cyclopropylamine moiety (DM); (ii) the identification of the specific P450 isoforms and non-CYP enzymes responsible for reactive metabolite formation; and, in particular, (iii) the investigation of the oxidative metabolism of DM by MPO.

Materials and Methods

Chemicals and Instruments. Human liver microsomes (HLMs) (pooled from 50 livers) were purchased from Xenotech, LLC (Kansas, KS). cDNA-expressed human P450 enzymes, flavin monooxygenase 3 (FMO3), MAO-A, and MAO-B, expressed from either baculovirus-infected insect cells or human lymphoblast cells, were purchased from BD Gentest Corp. (Woburn, MA). MPO (from human leukocyte, 220 units/mg protein) was obtained from Calbiochem (La Jolla, CA). HRP (type X, 291 units/mg protein), GSH, and catalase (11600 units/mg solid) were purchased from Sigma Chemical Corp. (St. Louis, MO). All other reagents, purchased from Sigma or Aldrich (Milwaukee, WI), were of the highest grade available unless otherwise noted. Routine ^{1}H spectra were obtained on a Varian Mercury Plus 300 (300 MHz, 75.4 MHz for ^{13}C) spectrometer. Chemical shifts are reported in parts per million (ppm) referenced to residual partially deuterated solvent peaks, and coupling constants are given in hertz (Hz). The LC/MS and LC/MS/MS analysis were conducted on a Thermo-Finnigan LCQ classic ion trap mass spectrometer with an electrospray ionization source and a Waters 2695 Separations Module using a Phenomenex Gemini C$_{18}$ (2.0 mm × 250 mm) column. Parameters for ESI were as follows: capillary temperature, 200 °C; spray voltage, 4.2 kV;

Scheme 2. Alternative Mechanism for P450-Mediated Oxidation of Cyclopropylamine to Reactive Intermediates by *N*-HAT Mechanism

capillary voltage, 7.0 V; sheath gas flow rate (nitrogen), 80 arb; and auxiliary gas flow rate (nitrogen), 20 arb.

Synthesis of 1-(Pyridin-2-yl)-2,5-dihydro-1*H*-pyrrole-3-carb-aldehyde—The α,β-Unsaturated Aldehyde M₁. A solution of 1α,5α,6α-3-(pyridin-2-yl)-6-amino-3-azabicyclo[3.1.0]hexane [Figure 1, DM (*19*)] (70 mg, 0.4 mmol) in H₂O/MeOH (2:1, 6 mL) was treated with K₃Fe(CN)₆ (790 mg, 2.40 mmol, 6 equiv). The pH of the reaction mixture was adjusted to 9 by 1 M NaOH, and the reaction was stirred at room temperature for 5 h. The aqueous phase was extracted with EtOAc twice. The combined organic layer was dried over anhydrous Na₂SO₄ and filtered. The solvent was evaporated, and the product was purified by flash chromatography (CHCl₃/acetone, 2:1). ESI-MS: $[M + H]^+$ = 175.0. ¹H NMR (300 MHz, CDCl₃): δ ppm 9.77 (s, 1H), 8.12 (dd, *J* = 5.1, 1.8 Hz, 1H), 7.44 (m, 1H), 6.96 (m, 1H), 6.56 (dd, *J* = 7.2, 5.1 Hz, 1H), 6.34 (d, *J* = 8.7 Hz, 1H), 4.54 (dt, *J* = 4.8, 2.4 Hz, 2H), 4.34 (dt, *J* = 5.1, 1.8 Hz, 2H). ¹³CNMR (75 MHz, CDCl₃) δ ppm 187.7, 148.5, 145.1, 142.8, 137.7, 112.6, 106.4, 54.8, 51.0.

Incubations with HLMs. The synthesized DM of TVX was incubated with HLMs to monitor the formation of M₁. Incubations containing 200 μM DM, 2.39 mM NADPH, 6 mM MgCl₂, and 2 mg/mL HLMs in 0.1 M potassium phosphate buffer (pH 7.4) with 1 mM EDTA were incubated in a dri-bath at 37 °C for 60 min. The final concentration of acetonitrile from DM stock solutions was no greater than 1%. Reactions were stopped by the addition of an equal volume of CH₃CN, vortex-mixed, and centrifuged at 14000*g* for 5 min. The resulting supernatant was used for all successive LC/MS and LC/MS/MS analysis. Incubations lacking microsomes or NADPH or DM served as negative controls. Incubations were also done with an additional 2 mM GSH to look for the presence of conjugated species.

Incubations with Microsomes Containing cDNA-Expressed Enzymes. Incubations with P450 3A4 were done using lymphoblast-expressed enzymes. All others were performed using baculovirus-expressed enzymes. Incubations were prepared as described above for HLMs, except that 40 pmol/mL of P450 enzymes or 0.4 mg/mL FMO3 (FMO3 was preincubated with DM for 3 min in ice before adding NADPH) was used. The following is a list of human cDNA-expressed enzymes utilized in this study: 1A1, 1A2, 2C9, 2C19, 2D6, 2E1, 3A4, and FMO3. Incubations with MAO-A and MAO-B containing 200 μM DM and 0.04 mg/mL MAO-A or MAO-B in 0.1 M potassium phosphate buffer (pH 7.4) were also performed, and the samples were processed as described above for HLMs.

Incubations with HRP and MPO. The peroxidase-mediated metabolism of the DM (200 μM) was studied using HRP (1 unit/mL) or MPO (1 unit/mL) in 0.1 M potassium phosphate buffer (pH 7.4), and the reaction was initiated by addition of H₂O₂ (0.22 mM). Following incubation at 37 °C for 60 min, the reaction was terminated, and the samples were processed as described above for HLMs. Incubations that lacked peroxidases served as negative controls. MPO-mediated oxidations were carried out in both the presence and the absence of 0.4 M KCl. Incubations were also done with an additional 2 mM GSH or 2 mM 4-bromobenzyl mercaptan to look for the presence of thiol-conjugated species.

Identification of Reactive Metabolites—α,β-Unsaturated Aldehyde. Metabolites were identified by positive electrospray LC/MS/MS analysis. Supernatant from in vitro incubations were introduced into the mass spectrometer using Phenomenex Gemini C₁₈ (2.0 mm × 250 mm, 5 μm) column. The mobile phase consisted of 0.03% aqueous NH₄OH (solvent A) and 0.03% NH₄OH in acetonitrile (solvent B), and the gradient was as follows: 0 min, 2% B; 4 min, 40% B; 4.5 min, 80% B; 10 min, 100% B; 15 min, 100% B; 16 min, 2% B; and 20 min, 2% B. The flow rate was 200 μL/min. 4-Bromobenzyl mercaptan adduct from MPO (with Cl⁻) incubation was also isolated by HPLC using the above conditions. Both the α,β-unsaturated aldehyde and its thiol adduct were reduced by NaBH₄ to confirm the existence of an aldehyde functional group.

**Figure 2.** HLMs and cDNA-expressed enzyme (P450s, FMO3, and MAO-A/B) metabolism of DM.

Time-Dependent Inactivation of MPO by the DM. Primary incubation mixtures containing 0.1 M potassium phosphate buffer, pH 7.4, 0.4 M KCl, 10 μM DM, and 1 unit/mL MPO were prewarmed at 37 °C for 2 min, and the reaction was initiated by the addition of H_2O_2 (0.22 mM). Control incubations were performed in the absence of DM. After preincubation for 0 or 15 min, 100 μM procainamide was added to the preincubation reaction mixtures. Aliquots were removed from the incubation mixtures, and the reaction was quenched at various time points by the addition of acetonitrile and an appropriate internal standard. The amount of 3-Cl procainamide formation was determined by integrating the mass chromatogram peaks using Xcalibur.

Inhibition Study of P450 1A2 by the DM of TVX. Incubations containing 200 μM DM, 2.39 mM NADPH, 6 mM MgCl$_2$, and 40 pmol/mL P450 1A2 in 0.1 M potassium phosphate buffer (pH 7.4) with 1 mM EDTA were preincubated in a dri-bath at 37 °C for 15 min. Control incubations were performed in the absence of DM. Then, 60 μM riluzole was added to the preincubation reaction mixtures. Aliquots were removed from the incubation mixtures, and the reaction was quenched at various time points by the addition of acetonitrile and an appropriate internal standard. The amount of *N*-hydroxy riluzole formation was determined by integrating the mass chromatogram peaks using Xcalibur.

Results

Metabolism of the DM of TVX by HLMs and cDNA-Expressed P450s, FMO3, and MAO-A/B. NADP(H)-dependent biotransformation of DM by HLMs produced no product corresponding to the proposed α,β-unsaturated aldehyde (MH$^+$, m/z 175) and the corresponding GSH conjugate (MH$^+$, m/z 482). Neither the reduced alcohol nor the oxidized carboxylic acid forms of M$_1$ and its GSH conjugate were detected. Incubations were then carried out with a number of commercially available cDNA-expressed human P450 isoenzymes (1A1, 1A2, 2C9, 2C19, 2D6, 2E1, and 3A4). The data (Figure 2) demonstrate that among the six major liver P450 enzymes (1A2, 2C9, 2C19, 2D6, 2E1, and 3A4), only P450 1A2 generated the reactive metabolite M$_1$ with an MH$^+$ ion at m/z 175. P450 1A1, which shows some homology to P450 1A2 but is expressed largely in extrahepatic tissue such as lung, was also found to produce M$_1$ to a lesser extent. No M$_1$ formation was detected from FMO3 or MAO-A/B incubations. The concentration of M$_1$ formed in the incubation with P450 1A2 (40 pmol/mL) and DM (200 μM) for 1 h was calculated to be 0.24 μM by comparison with the calibration curve of synthetic M$_1$ and internal standard.

Metabolism of DM of TVX by Peroxidases. HRP and MPO enzymes were used to catalyze the oxidative metabolism of DM. Control was performed under identical conditions in the absence
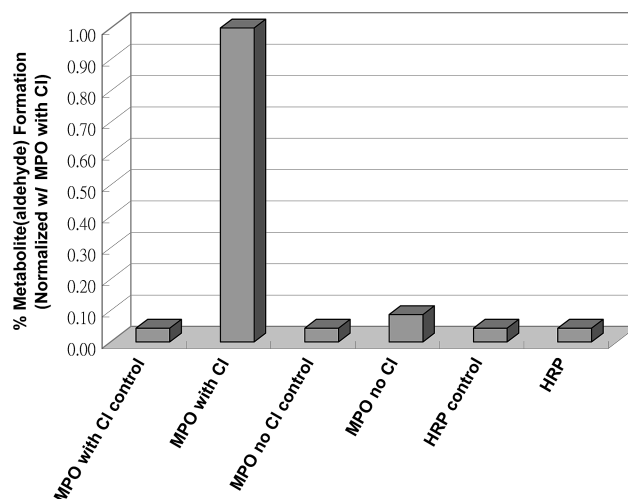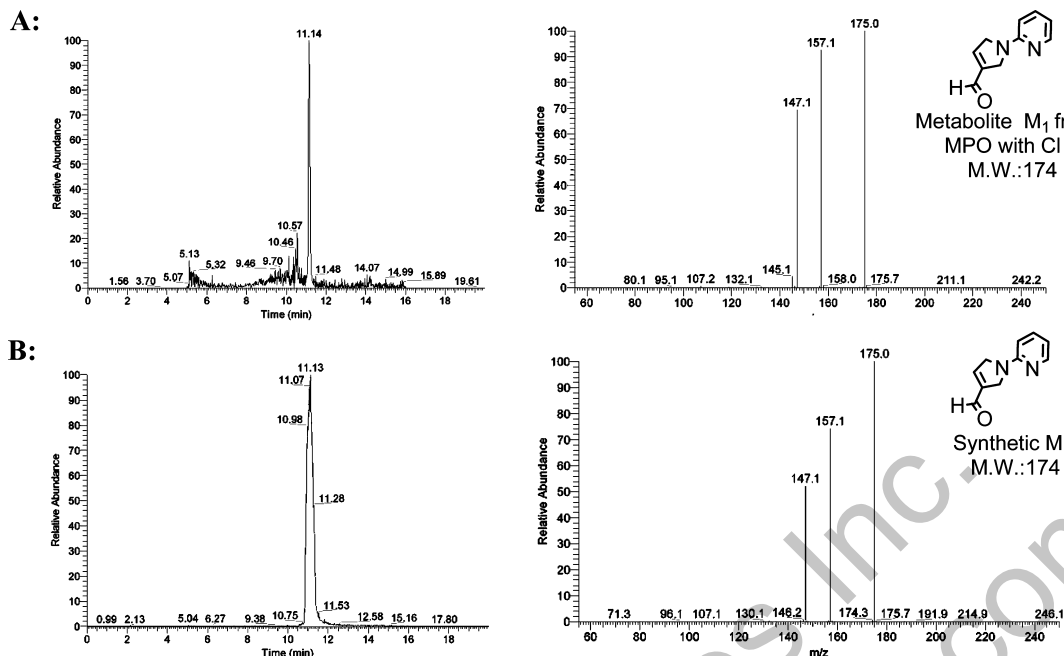

Figure 3. MPO and HRP metabolism of DM.

of the metabolizing enzymes. MPO incubations were done in both the presence and the absence of chloride. Data (Figure 3) showed that incubation with MPO (with Cl$^-$) produced a significant amount of reactive metabolite M$_1$, while incubation with MPO in absence of chloride or with HRP produced a trace amount or no α,β-unsaturated aldehyde as compared to the respective control. All of the control experiments produced small amounts of M$_1$, which may come from the background oxidation by H_2O_2. The concentration of M$_1$ formed in incubation with MPO (30 pmol/mL) and DM (200 μM) for 1 h was calculated to be 1.20 μM by comparison with the calibration curve of synthetic M$_1$ and internal standard.

Structural Characterization of Reactive Metabolite M$_1$ by LC-MS and MS/MS Analyses. The reactive metabolite M$_1$ was produced in relatively high amounts by MPO in the presence of chloride ion among all of the incubations tested. This source was used for all of the following structure characterization experiments. LC/ESI-MS/MS analysis revealed the formation of M$_1$ with MH$^+$ at m/z 175 from incubation with MPO in the presence of chloride ion. Metabolite M$_1$ eluted at 11.14 min and gave rise to fragments $m/z = 157$ (loss of H_2O) and $m/z = 147$ (loss of CO) (Figure 4A). M$_1$ was independently synthesized by chemical methods. LC/MS analysis of synthetic M$_1$ revealed that it eluted at 11.13 min and yielded the same fragment ions as metabolite M$_1$ (Figure 4B). When M$_1$ from the MPO incubation (with Cl$^-$) was reduced by NaBH$_4$, the original peak with MH$^+$ at m/z 175 ($t_R = 11.14$ min) disappeared, and a new peak with MH$^+$ at m/z 177 ($t_R = 10.31$ min) appeared (Figure 5A). This M + 2 peak, corresponding to the reduction of aldehyde to alcohol, supports the existence of an aldehyde functional group in the metabolite M$_1$. The NaBH$_4$ reduction experiment was repeated on the synthetic M$_1$, and it was found that the peak with MH$^+$ at m/z 175 ($t_R = 10.13$ min) disappeared too, and the corresponding peak with MH$^+$ at m/z 177 eluted at the same retention time ($t_R = 10.32$ min) as the reduced product from metabolite M$_1$ (Figure 5B). Incubations with MPO (with Cl$^-$) were also made with an additional thiol scavenger to look for the presence of conjugated species. GSH, a biologically relevant trapping agent, was used first. The conjugate was observed by LC-MS analysis, but it was found to elute at the solvent front, which made it difficult to separate from salt and the higher concentration of the trapping reagent, limiting MS/MS analysis. To solve this problem, 4-bromobenzyl mercaptan was used to yield a conjugate with a longer retention time. The corresponding 4-bromobenzyl mercaptan conjugate with metabolite M$_1$ from the incubation with MPO (with Cl$^-$)

Insights into Trovafloxacin-Induced Hepatotoxicity

Chem. Res. Toxicol., Vol. 21, No. 3, 2008 **715**

Figure 4. (A) Top left: LC chromatogram with mass filter m/z 175 showing peak ($t_R = 11.14$ min) associated with metabolite M_1 from MPO incubation (with Cl^-). Top right: MS/MS spectrum of metabolite M_1 from MPO incubation (with Cl^-). (B) Bottom left: LC chromatogram with mass filter m/z 175 showing peak ($t_R = 11.13$ min) associated with synthetic standard M_1. Bottom right: MS/MS spectrum of synthetic standard M_1.

was observed with MH^+ at m/z 377/379 that matched the isotope distribution pattern of the bromine atom. Reduction of this conjugate by $NaBH_4$ generated the corresponding $M + 2$ peak with MH^+ at m/z 379/381 (Figure 6). The thiol conjugation and $NaBH_4$ reduction were also carried out for the synthetic M_1. The results were in agreement with those obtained with the metabolite M_1. Furthermore, these structural characterization experiments were repeated with P450 1A2-produced metabolite and gave the exact same results.

Time-Dependent Inhibition of MPO by the DM of TVX. Procainamide is a substrate of MPO and can be oxidized by MPO in the presence of chloride ion to reactive *N*-chloroprocainamide. The reactive *N*-chloroprocainamide spontaneously rearranges to the stable product 3-chloroprocainamide (*20*). The inhibition mode of DM toward MPO was tested by using procainamide as a substrate. MPO was preincubated with DM for different periods of time, and then, procainamide was added. Following addition, the formation of 3-chloroprocainamide was tested at various time points. Without preincubation, MPO metabolism of procainamide in the absence and presence of DM of TVX showed that the presence of DM had no effect of 3-chloroprocainamide formation. However, preincubation of MPO with DM for 15 min, followed by addition of procainamide, led to a considerable decrease in 3-chloroprocainamide formation as compared to a control in which the preincubation was performed in the absence of DM (Figure 7). This suggested that the inhibition of MPO by DM was time-dependent and that DM served as a suicide inhibitor of MPO in the presence of chloride ion.

Inhibition Study of P450 1A2 by DM of TVX. Riluzole, 2-amino-6-(trifluoromethoxy)benzothiazole, is predominantly metabolized by P450 1A2 in human hepatic microsomes to *N*-hydroxy riluzole (*21*). P450 1A2 was preincubated with DM for 15 min, and the controls were done in a similar manner except that DM was omitted. Riluzole was added subsequently, and the formation of *N*-hydroxyl riluzole was tested at various time points.

The results (Figure 8) showed that preincubation of P450 1A2 with DM at 200 μM for 15 min, followed by the addition of riluzole, led to an increase in *N*-hydroxyl riluzole formation as compared to the control in which the preincubation was performed in the absence of the DM. However, preincubation of P450 1A2 with tacrine, a P450 1A2 substrate (*22*), at 200 μM results in a normal competitive inhibition as compared to the control. Although the exact reason for why DM increases the oxidation of riluzole by P450 1A2 is unclear at this moment, DM has been demonstrated to have no inhibition of P450 1A2 at 200 μM.

Discussion

The mechanism responsible for the hepatotoxicity of trovafloxacin has remained unresolved since the observation of drug-related hepatotoxicity in the clinic. TVX possesses two substructural elements that have the potential to generate reactive intermediates: a cyclopropylamine moiety and a difluoroanilino system. Cyclopropylamines have been widely applied as mechanistic probes for oxidative enzymes and were reported to generate reactive intermediates on metabolism by P450s, HRP, and MAOs (*8–16*). A DM of TVX was synthesized in our laboratories to examine the potential for oxidation of the cyclopropylamine substructure in TVX to reactive intermediates without interference from the difluoroanilino substructure. In vitro metabolism of the molecular model containing the cyclopropylamine moiety with P450s, FMO3, and MAO-A/B revealed that only P450 1A2 could oxidize DM to the reactive α,β-unsaturated aldehyde M_1. However, no α,β-unsaturated aldehyde or the corresponding thiol conjugate was detected from incubation with HLMs. The reduced alcohol and oxidized carboxylic acid forms were also investigated; however, neither were detected. One possible explanation is that HLMs are a complicated mixture of a variety of enzymes that can trap the small amount of α,β-unsaturated aldehyde produced by P450 1A2, thus making it undetectable. In the absence of chloride ion, MPO had a low ability to oxidize DM similar to HRP.
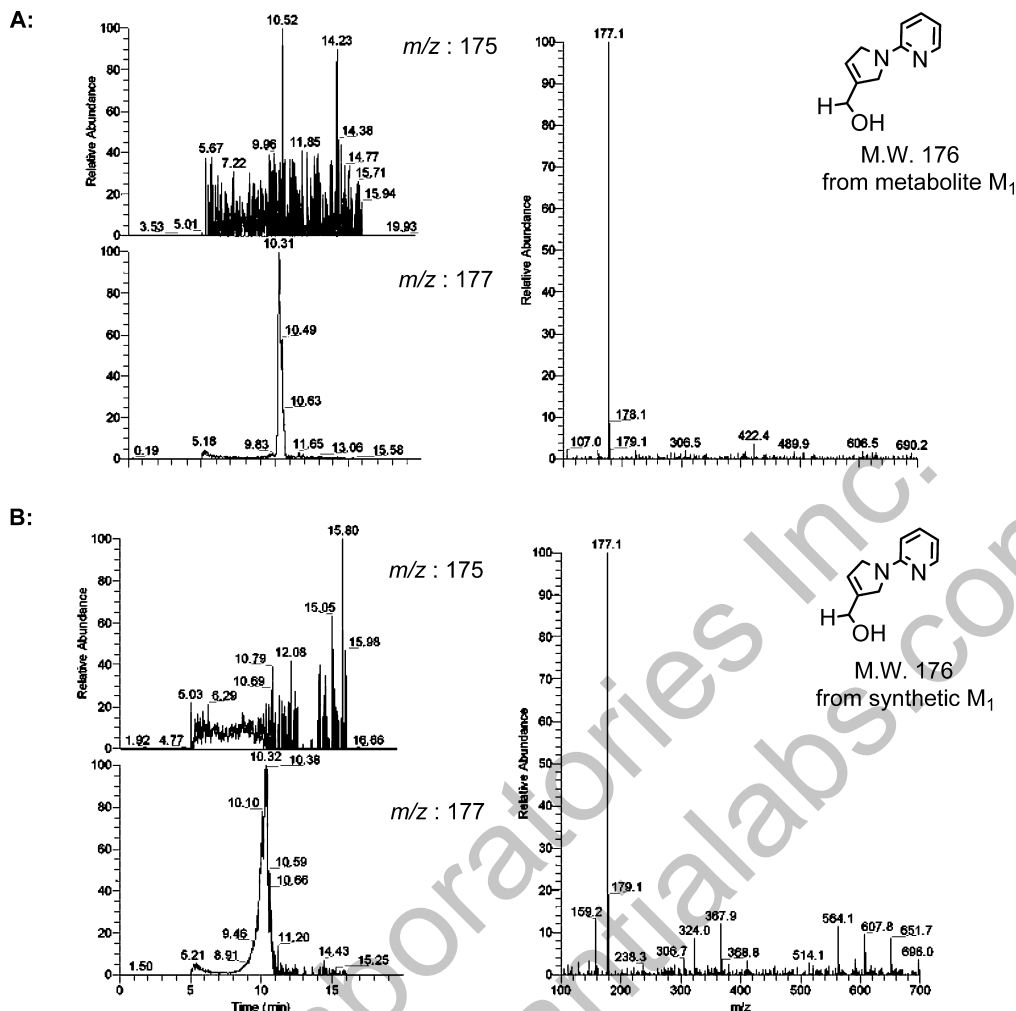
Figure 5. (A) Top left: LC chromatogram showing disappearance of the peak with m/z 175 (t_R = 11.14 min from Figure 4A, left panel) and appearance of a new peak (t_R = 10.3 min) with m/z 177 after reducing metabolite M_1 from MPO incubation (with Cl^-) by $NaBH_4$. Top right: MS spectrum of the corresponding new peak (t_R = 10.31 min). (B) Bottom left: LC chromatogram showing disappearance of the peak with m/z 175 (t_R = 11.13 min from Figure 4B, left panel) and appearance of a new peak (t_R = 10.32 min) with m/z 177 after reducing synthetic standard M_1 by $NaBH_4$. Bottom right: MS spectrum of the corresponding new peak (t_R = 10.32 min).
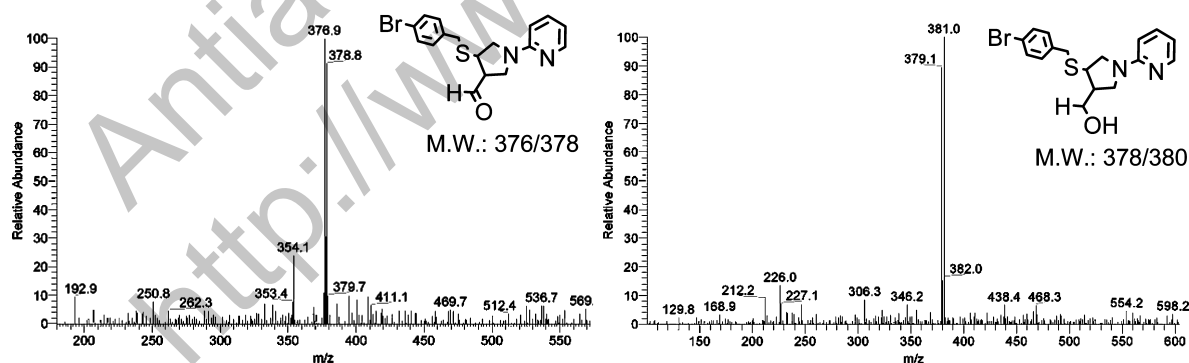
Figure 6. Left panel: MS spectrum of 4-bromobenzyl mercaptan conjugate with M_1 from MPO incubation (with Cl^-), which matches bromine atom isotope distribution form with m/z = 377/379 (1:1). Right panel: MS spectrum of corresponding $NaBH_4$ reduced product of thiol conjugate with m/z at 379/381.

While in the presence of chloride ion, MPO oxidized DM to α,β-unsaturated aldehyde in the largest amount among all of the tested incubations. The structure of the reactive intermediate has been confirmed by LC-MS/MS analysis and also by comparison with a synthetic standard. DM showed no inhibition of P450 1A2 at a concentration as high as 200 μM, while it was proved to be a suicide inhibitor to MPO in the presence of chloride ion at 10 μM.

The most meaningful finding from these studies is that nonliver enzyme MPO oxidized cyclopropylamine to the reactive α,β-unsaturated aldehyde, which may contribute to the hepatotoxicity of TVX. MPO is one of the major enzymes of the antimicrobial system of mammalian neutrophils. The microbicidal activity of MPO comes from its ability to catalyze the peroxide-dependent oxidation of halide ions (physiological plasma concentrations: Cl^-, 100–140 mM; Br^-, 20–100 μM)
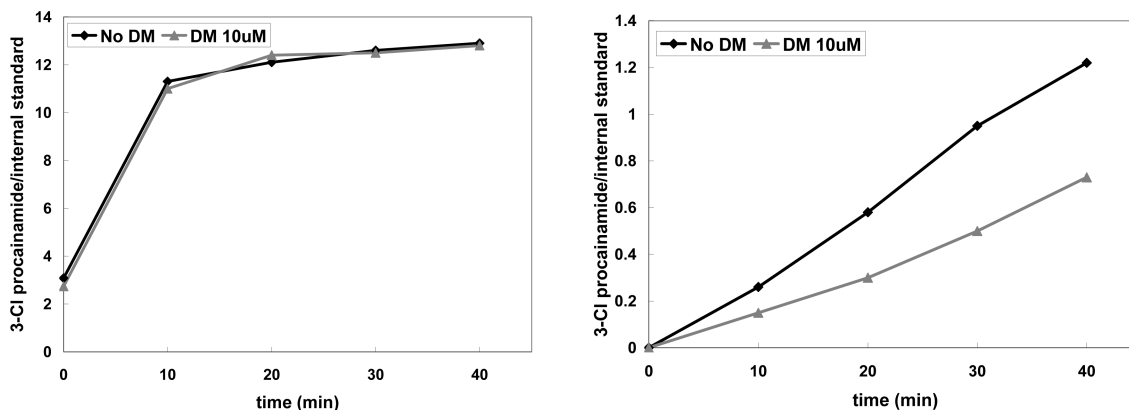
Figure 7. 3-Cl procainamide production from MPO incubation of procainamide in the presence of chloride ion at 37 °C in the absence (♦) and presence (▲) of 10 μM DM. Left panel, 0 min of preincubation; right panel, 15 min of preincubation.
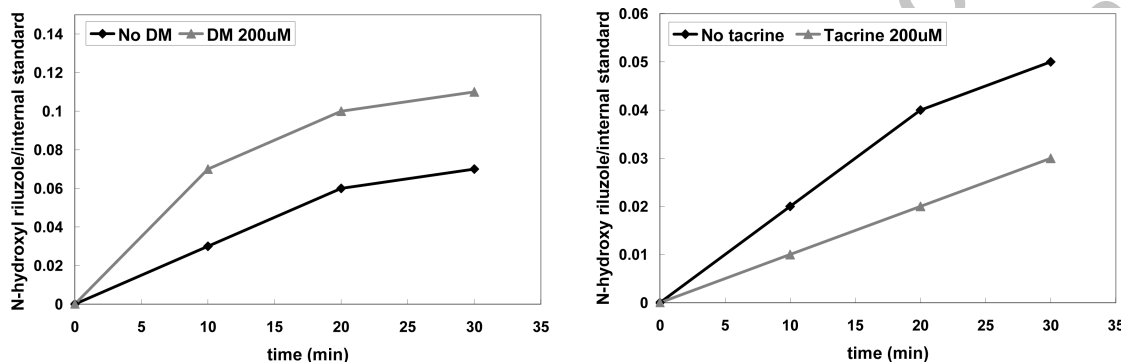

Figure 8. *N*-Hydroxy riluzole production from incubation with P450 1A2 and riluzole at 37 °C. Left panel: in the absence (♦) and presence (▲) of 200 μM DM (15 min of preincubation). Right panel: in the absence (♦) and presence (▲) of 200 μM tacrine (15 min of preincubation).

and thiocyanate to hypohalous acids and hypothiocyanate, which are effective antimicrobial agents (*23*). However, the production of these reactive oxidants in inappropriate quantities, locations, or time in the body can lead to significant tissue damage (*24*). In animal model studies, cotreatment of rats with nonhepatotoxic doses of bacterial lipopolysaccharide (LPS) and TVX leads to liver neutrophil (PMN) accumulation and activation. This response may be responsible for the hepatotoxicity, which was

not observed with either agent alone in rats. Prior depletion of PMN attenuated the liver injury confirming the role of PMN in the hepatotoxicity induced by LPS/TVX (*17*). Besides TVX, the idiosyncratic hepatotoxicities of halothane, monocrotaline, acetaminophen, ranitidine, and chloropromazine have been reported to be predictable in the LPS−drug idiosyncrasy model. One hypothesis for the pathogenesis of hepatic IDRs is that, in certain individuals, underlying inflammation results in the

Scheme 3. Proposed Mechanism for MPO-Mediated Oxidation of DM
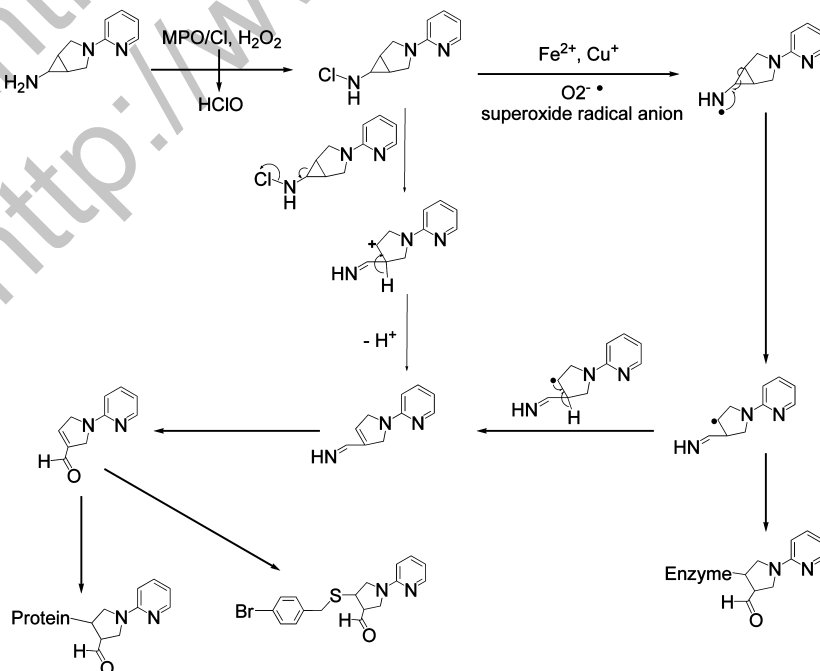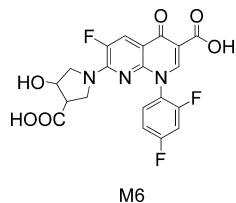
Figure 9. Chemical structure of phase I oxidative metabolite "M6" of TVX.

sensitization of the liver, such that injury occurs from an agent that typically would not cause hepatotoxicity at a therapeutic dose (*17*). For halothane (*25*) and acetaminophen (*26*), the infiltration of PMN into the liver has been reported to have no influence on the drug bioactivation. However, for TVX, the recruitment of PMN into the liver and its activation to release MPO may contribute significantly to the oxidization of the cyclopropylamine moiety to a reactive α,β-unsaturated aldehyde, aggravating the tissue injury. The exact mechanism for how P450 1A2 and MPO oxidation may contribute to the ultimate hepatotoxicity of TVX is still under investigation.

We have proposed possible mechanisms for MPO oxidation of cyclopropylamine to the α,β-unsaturated aldehyde, M_1, based on the reported mechanism for MPO oxidation of acyclic amines (Scheme 3). MPO utilizes H_2O_2 to oxidize chloride ion to generate the potent oxidant, hypochlorous acid, which will then oxidize the primary amine to yield an unstable, reactive chloramine. The chloramine can subsequently degrade via one-electron reduction by metal ions (Fe^{2+}, Cu^+) or the superoxide radical anion ($O_2^{-\bullet}$) to form a nitrogen-centered radical (RNH$^\bullet$) (*27, 28*). Concurrent with P450 oxidation, the neutral aminyl radical can lead to either enzyme inactivation or α,β-unsaturated aldehyde formation. Alternatively, the chloramine can undergo a two-electron ionization process—possibly mediated by a metal ion Lewis acid—followed by deprotonation to produce the unsaturated imine intermediate. Unfortunately, this model system does not shed additional light on the issue of SET vs *N*-HAT/ *C*-HAT oxidation of amines by P450 enzymes or other oxidative enzymes.

In vivo metabolism studies with TVX showed that phase II metabolism (glucuronidation, *N*-acetylation, and *N*-sulfation) provided the major clearance pathway for the compound; however, lesser amounts of phase I metabolism were also observed (*29, 30*). The oxidized hydroxycarboxylic acid metabolite M6 (Figure 9) confirmed the oxidation of the cyclopropylamine substructure of TVX (*29*). The hydroxycarboxylic acid metabolite M6 can be formed by the addition of water to the carbocation intermediate in the two-electron oxidation pathway (Scheme 3) or to the α,β-unsaturated aldehyde by Michael addition, followed by the oxidation of aldehyde to carboxylic acid. Furthermore, DM showed no inhibition of P450 1A2, which is consistent with the observation that TVX showed no interference of theophylline clearance, as monitored by P450 1A2 (*31, 32*). Although MPO is not a liver enzyme, neutrophils, which release MPO, have been associated with idiosyncratic hepatotoxic drug reactions of a variety of drugs in the LPS–drug idiosyncrasy model. Thus, some drugs may be oxidized by MPO to reactive intermediates that can form covalent adducts with hepatic proteins, resulting in damage to liver tissue. It is additionally possible that low levels of reactive intermediate formation by endogenous liver enzymes, as illustrated by the oxidation of DM by P450 1A2, may lead to limited tissue damage that results in the recruitment of neutrophils and subsequent amplification of the damage by MPO-mediated reactive intermediate production. In summary, these results lend

support to the hypothesis that TVX-induced hepatotoxicity can be mediated by oxidation of the cyclopropylamine substructure to reactive intermediates.

References

(1) Gooding, B. B., and Jones, R. N. (1993) In vitro antimicrobial activity of CP-99,219, a novel azabicyclo-naphthyridone. *Antimicrob. Agents Chemother. 37*, 349–353.

(2) Spangler, S. K., Jacobs, M. R., and Appelbaum, P. C. (1994) Activity of CP-99,219 compared with those of ciprofloxacin, grepafloxacin, metronidazole, cefoxitin, piperacillin, and piperacillin-tazobactam against 489 anaerobes. *Antimicrob. Agents Chemother. 38*, 2471–2476.

(3) Coque, T. M., Singh, K. V., and Murray, B. E. (1996) Comparative in-vitro activity of the new fluoroquinolone trovafloxacin (CP-99,219) against gram-positive cocci. *J. Antimicrob. Chemother. 37*, 1011–1016.

(4) Teng, R., Harris, S. C., and Nix, D. E. (1995) Pharmacokinetics and safety of trovafloxacin (CP-99,219), a new quinolone antibiotic, following administration of single oral doses to healthy male volunteers. *J. Antimicrob. Chemother. 36*, 385–394.

(5) Bertino, J., Jr., and Fish, D. (2000) The safety profile of the fluoroquinolones. *Clin. Ther. 22*, 798–817.

(6) U.S. Food and Drug Administration Website. Public Health Advisory. Trovan (trovafloxacin/alatrofloxacin mesylate). June 9, 1999. Available at http://www.fda.gov/cder/news/trovan.

(7) Ball, P., Mandell, L., Niki, Y., and Tillotson, G. (1999) Comparative tolerability of the newer fluoroquinolone antibacterials. *Drug Saf. 21*, 407–421.

(8) Macdonald, T. L., Zirvi, K., Burka, L. T., Peyman, P., and Guengerich, F. P. (1982) Mechanism of cytochrome P-450 inhibition by cyclopropylamines. *J. Am. Chem. Soc. 104*, 2050–2052.

(9) Guengerich, F. P., and Macdonald, T. L. (1984) Chemical mechanisms of catalysis by cytochromes P-450: A unified view. *Acc. Chem. Res. 17*, 9–16.

(10) Bondon, A., Macdonald, T. L., Harris, T. M., and Guengerich, F. P. (1989) Oxidation of cycloalkylamines by cytochrome P-450. *J. Biol. Chem. 264*, 1988–1997.

(11) Cerny, M. A., and Hanzlik, R. P. (2006) Cytochrome P450-catalyzed oxidation of *N*-benzyl-*N*-cyclopropylamine generates both cyclopropanone hydrate and 3-hydroxypropionaldehyde via hydrogen abstraction, not single electron transfer. *J. Am. Chem. Soc. 128*, 3346–3354.

(12) Silverman, R. B., and Hiebert, C. K. (1988) Inactivation of monoamine oxidase A by the monoamine oxidase B inactivators 1-phenylcyclopropylamine, 1-benzylcyclopropylamine, and *N*-cyclopropyl-α-methylbenzylamine. *Biochemistry 27*, 8448–8453.

(13) Silverman, R. B. (1995) Radical ideas about monoamine oxidase. *Acc. Chem. Res. 28*, 335–342.

(14) Zhong, B., and Silverman, R. B. (1997) Identification of the active site cysteine in bovine liver monoamine oxidase B. *J. Am. Chem. Soc. 119*, 6690–6691.

(15) Vintem, A. P., Price, N. T., Silverman, R. B., and Ramsay, R. R. (2005) Mutation of surface cysteine 374 to alanine in monoamine oxidase A alters substrate turnover and inactivation by cyclopropylamines. *Bioorg. Med. Chem. 13*, 3487–3495.

(16) Sayre, L. M., Naismith, R. T., Bada, M. A., Li, W., Klein, M. E., and Tennant, M. D. (1996) trans-2-Phenylcyclopropylamine is a substrate for and inactivator of horseradish peroxidase. *Biochim. Biophys. Acta-Protein Struct. Mol. Enzymol. 1296*, 250–256.

(17) Waring, J. F., Liguori, M. J., Luyendyk, J. P., Maddox, J. F., Ganey, P. E., Stachlewitz, R. F., North, C., Blomme, E. A., and Roth, R. A. (2006) Microarray analysis of lipopolysaccharide potentiation of trovafloxacin-induced liver injury in rats suggests a role for proinflammatory chemokines and neutrophils. *J. Pharmacol. Exp. Ther. 316*, 1080–1087.

(18) Ball, P., and Ed, F. (2003) Efficacy and safety of levofloxacin in the context of other contemporary fluoroquinolones: a review. *Curr. Ther. Res. 64*, 646–661.

(19) Sun, Q., Zhu, R., Jr., and Macdonald, T. L. (2007) Mechanisms of trovafloxacin hepatotoxicity: Studies of a model cyclopropylamine-containing system. *Bioorg. Med. Chem. Lett. 17*, 6682–6686.

(20) Uetrecht, J. P., and Zahid, N. (1991) N-Chlorination and oxidation of procainamide by myeloperoxidase: Toxicological implications. *Chem. Res. Toxicol. 4*, 218–222.

(21) Sanderink, G.-J., Bournique, B., Stevens, J., Petry, M., and Martinet, M. (1997) Involvement of human P450 1A isoenzymes in the metabolism and drug interactions of riluzole in vitro. *J. Pharmacol. Exp. Ther. 282*, 1465–1472.

(22) Spaldin, V., Madden, S., Adams, D. A., Edwards, R. J., Davies, D. S., and Park, B. K. (1995) Determination of human hepatic cytochrome P4501A2 activity in vitro use of tacrine as an isoenzyme-specific probe. *Drug Metab. Dispos. 23*, 929–934.

(23) Klebanoff, S. J. (1970) Myeloperoxidase: Contribution to the microbicidal activity of intact leukocytes. *Science 169*, 1095–1097.

(24) Pattison, D. I., and Davies, M. J. (2006) Reactions of myeloperoxidase-derived oxidants with biological substrates: Gaining chemical insight into human inflammatory diseases. *Curr. Med. Chem. 13*, 3271–3290.

(25) You, Q., Cheng, L., Reilly, T. P., Wegmann, D., and Ju, C. (2006) Role of neutrophils in a mouse model of halothane-induced liver injury. *Hepatology 44*, 1421–1431.

(26) Liu, Z.-X., Han, D., Gunawan, B., and Kaplowitz, N. (2006) Neutrophil depletion protects against murine acetaminophen hepatotoxicity. *Hepatology 43*, 1220–1230.

(27) Hawkins, C. L., and Davies, M. J. (2005) The role of reactive *N*-bromo species and radical intermediates in hypobromous acid-induced protein oxidation. *Free Radical Biol. Med. 39*, 900–912.

(28) Hawkins, C. L., and Davies, M. J. (2001) Hypochlorite-induced damage to nucleosides: Formation of chloramines and nitrogen-centered radicals. *Chem. Res. Toxicol. 14*, 1071–1081.

(29) Dalvie, D. K., Khosla, N. B., Navetta, K. A., and Brighty, K. E. (1996) Metabolism and excretion of trovafloxacin, a new quinolone antibiotic, in Sprague-Dawley rats and beagle dogs. Effect of bile duct cannulation on excretion pathways. *Drug Metab. Dispos. 24*, 1231–1240.

(30) Vincent, J., Teng, R., Dalvie, D. K., and Friedman, H. L. (1998) Pharmacokinetics and metabolism of single oral doses of trovafloxacin. *Am. J. Surg. 176* (6A Suppl.), 8S–13S.

(31) Vincent, J., Teng, R., Dogolo, L. C., Willavize, S. A., and Friedman, H. L. (1997) Effect of trovafloxacin, a new fluoroquinolone antibiotic, on the steady-state pharmacokinetics of theophylline in healthy volunteers. *J. Antimicrob. Chemother. 39* (Suppl. B), 81–86.

(32) Ha, H. R., Chen, J., Freiburghaus, A. U., and Follath, F. (1995) Metabolism of theophylline by cDNA-expressed human cytochromes P-450. *Br. J. Clin. Pharmacol. 39*, 321–326.

TX7003085